

Fundamental Noise Studies in Flame Atomic Magneto-Optic Rotation and Atomic Absorption Spectrometry*

Ahmet T. İNCE

*Yeditepe University, Letters and Science Faculty,
Department of Physics, Üsküdar, İstanbul-TURKEY*

Richard D. SNOOK, John B. DAWSON

*Department of Instrumentation and Analytical Science,
University of Manchester Institute of Science & Technology,
PO Box 88, M60 1QD, Manchester-ENGLAND*

Received 17.12.1998

A study of inherent noise sources present in a purpose built flame atomic magneto-optic rotation (AMOR) spectrometer system was carried out with a view to identifying their sources. Two different optical configurations were employed, a crossed polariser and a 45° offset polariser configuration. The offset polariser configuration was operated in both an AMOR and atomic absorption (AA) mode for the noise measurements.

Two main interference frequencies were found to occur in all the optical measurement modes. An interference flame feature frequency (15.5 Hz -39.0 Hz) which arose from an “organ-pipe” effect in the gas flow through the flame cooling sheets. The second interference frequency (at 100 Hz) was thought to arise due to modulation of the analytes magneto-optic properties due to ripple on the electromagnet d.c. power supply. Photon noise and fluctuation noise were found to be present as background noise. The fluctuation noise was dominant at higher analyte concentrations.

The characteristics and origins of fluctuation noise are discussed and investigated for each measurement mode. The noise spectra of the conventional AA measurements were compared with those of the contemporary AMOR measurements, to ascertain any differences in noise power spectra which may affect the signal-to-noise ratio.

Key words: Atomic magneto-optic rotation spectrometer (AMORS), air-acetylene flame atomiser, Faraday configuration, fluctuation noise, offset polarisers, atomic absorption spectrometer.

Introduction

Atomic magneto-optic rotation spectroscopy (AMORS) is a fairly contemporary analytical spectroscopy technique similar to atomic absorption spectroscopy (AAS), but which relies on the rotation of plane polarised light by an analyte vapour. The AMOR analytical signal obtained is dependent on the analyte concentration.

* Part of this work was presented at the Biennial conference, July, 1992, Plymouth, England

Analytical spectroscopy involves analytical chemistry techniques, instrumentation and signal processing techniques. The desired parameters to be improved in analytical spectroscopy are detection limits, sensitivity and accuracy. The path to this goal is most often by improving chemical analysis techniques or instrumentation. Signal processing techniques are, however, just as significant in achieving this goal. More specifically, reducing the number of noise sources in measurements leads to an increase in the signal-to-noise ratio and hence to improvements in the desired parameters. This can only be carried out by identifying the sources of noise in these measurements and to investigate their origins.

In analytical spectroscopy noise is generated from the instrumental components or is the result of fluctuations and errors in any stage of the analytical measurement procedure. The whole measurement process can be characterised by observing its noise power spectra (NPS). The NPS indicates noise superimposed by the noise source (or device) onto the signal per unit frequency.

The two types of noise usually present on analytical spectroscopy NPS in a given bandwidth are photon noise, $N(p)$ and fluctuation noise, $N(f)$. The former arises from the light source and is an additive type of noise. It has the dependence $N(p) \propto \sqrt{I}$ where I is the light intensity^{1,2}. Fluctuation noise or $1/f$ noise generally arises from variations in the analyte concentration within the optical path. It is a multiplicative type of noise i.e., its amplitude increases linearly with analyte concentration. This proportional nature distinguishes it from photon noise. Fluctuation noise has a dependency, which has been fitted³ to equation 1.

$$N(f) = A \frac{\langle i^2 \rangle}{e^2} f^{-\beta} + c \quad (1)$$

Where A depends on analyte concentration, $\langle i^2 \rangle$ is the mean square photocurrent, e is the electronic charge, β is the fluctuation noise exponent and varies as $0.95 \leq \beta \leq 1.2$, c is the shot noise contribution $2\langle i \rangle / e$ with constant white noise. In this paper noise sources present in AMORS are investigated by investigating their NPS. The NPS found are then compared with those for atomic absorption mode measurements undertaken using the same instrumentation.

If an atomic vapour (produced for example by a flame or other atomiser) is placed under the influence of a magnetic field of sufficient strength, it exhibits optical activity, caused by the combined effect of birefringence and dichroism of the atomic vapour^{4,5}. If plane polarised resonance radiation propagates through the atomic vapour under these circumstances, its plane of polarisation is rotated. The degree of rotation may be detected as an analytical signal, whose intensity determines the degree of rotation if an appropriate optical detection system is employed. A polariser and analyser were employed for this purpose, the analyser was stationary and was set at an angle 90° relative to the polariser and the polariser was placed on a rotatable mount, at an angle $\Phi = 0^\circ$ to the plane of the analyser optical axis. This relative polariser orientation is called a crossed configuration, so that plane polarised light is not transmitted by the analyser unless the plane of polarisation of the resonance radiation from the polariser is rotated by the analyte atomic vapour, giving a component along the axis of the analyser. In this configuration the detected signal displays a quadratic dependence on analyte concentration, which adversely affects the detection limits⁶⁻⁸. A method of overcoming this quadratic dependence and improving the detection limits is to employ an offset polariser arrangement^{4,9-11} in which Φ is offset to 45° , by rotation of the polariser.

The AMOR spectrometer, designed for trace element analysis, was operated in the Faraday configuration. Three optical configurations of the spectrometer were investigated; an AMOR crossed polariser arrangement ($\Phi = 0^\circ$) AMOR offset polariser arrangement ($\Phi = 45^\circ$) and an atomic absorption arrangement ($\Phi = 45^\circ$), where the magnetic field was switched off. The NPS of AMORS and absorption measurements were analysed. Each operation mode or configuration will have differences in their NPS. These were

compared and contrasted to find noise contributions and interference frequencies which adversely affect the signal to noise ratios. The physical basis for the generation of the noise sources have been investigated and methods of removing or attenuating them are sought.

Experimental

Apparatus

The AMOR spectrometer is shown in Figure 1 and comprises a hollow cathode lamp source (HCL); radiation from the lamp is passed in turn through a Glan air prism, the air-acetylene flame and Rochon polariser to a 1 metre Czerny-Turner spectrometer of $8\text{\AA}/\text{mm}$ linear reciprocal dispersion (Hilger monospek 1000, Rank Hilger, Margate, Kent). The transmitted radiation is detected using an EMI photo multiplier tube, the output of which is fed to a current-to-voltage converter and subsequently to an oscilloscope, chart recorder or spectrum analyser (Hewlett Packard 3561A). The Glan-air prism is fixed to a rotatable mount and the flame is located between two water-cooled pole pieces of a d.c. electromagnet. This apparatus is described in detail elsewhere⁶, however the experimental operating conditions are listed in the Table.

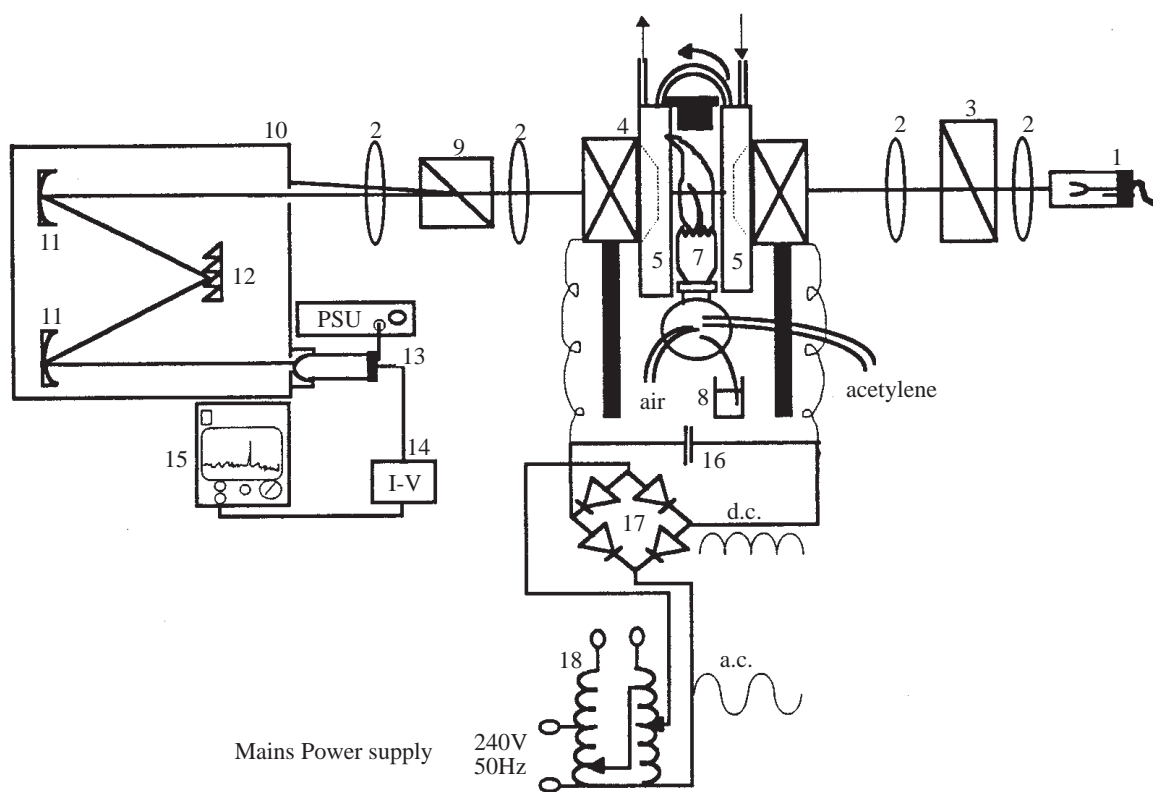


Figure 1. Experimental set-up for AMOR spectral measurement;

1 : Hollow cathode lamp, 2 : lenses, 3 : glan-air prisim, 4 : Electro-magnet solenoid coil, 5 : welded water cooling sheets (surrounding the flame), 6 : flame (air-acetylene) 7 : Nebuliser-burner assembly, 8 : sample, 9: Rochon prism, 10: Grating monochromator, 11: Concave mirror, 12: Diffraction grating, 13: photomultiplier tube, 14: current to voltage convertor, 15: Dynamic signal analyser, 16: Smoothing capacitor, 17: full-wave bridge rectifier, 18: Magnet power supply

Table Experimental Conditions

Analyte Dependent Parameters	Analytes	
	Mg	Cu
Wavelength/nm	285.1	324.7
Field strength/Tesla	0.55	0.2
Parameters common to Mg, Cu		
Monochromator	Rank Hilger, monospek	
r.l.d*/A°.mm ⁻¹	8	
grating spacing/lines.mm ⁻¹	1200	
Entrance and exit slit width/mm	0.5	
Polariser	Glan-air prism	
Analyser	Rochon prism	
Electromagnet	Laboratory constructed (water cooled)	
Maximum field strength/Tesla	0.8	
Coil current/Amp.	30	
Atomiser	Air-acetylene flame	
Air flow rate, L/min	3.19	
Acetylene flow rate, L/min	0.9	
Flame height ⁺ /cm	2.0	
Beam area on flame/cm ²	0.4	
Optical path length/mm	8	
Hollow cathode lamp applied current/mA	8	
Photomultiplier tube applied d.c. volt/V	800	
Nebuliser uptake/ml.min ⁻¹	8	
Spectrum analyser	Hewlett Packard 3561A, operating bandwidth of 0-100kHz	

*Linear reciprocal dispersion,

+Distance between the optical path and top of the flame burner

A stabilised power supply unit (P.S.U.) supplied the current to the HCL source. To produce the required magnetic fields of typically 0.05 T-0.8 T in a pole gap of 13 mm, a second P.S.U. supplied the current to the electromagnet via a full-wave bridge rectifier (60 Amp. SIL bridge 60/68, farnell). All measurements were carried out with an optical path passing through the air-acetylene flame (modified commercial design) which burns in the gap of the electromagnet. The flame head consisted of 8 fine slots, each 1 mm by 10 mm. Six of these slots were welded closed since they were outside the optical path, leaving two open slots, which extended across the optical path. The flame was observed to be approximately 10 mm in width and 20 mm in length. The burner was 85 mm in height, and was connected to a spray chamber and pneumatic nebuliser, the burner, spray chamber and nebuliser assembly was bolted onto a lab-jack, which served to vary the flame burner along the length of the cooling sheets. The voltage output of the detection system formed the input to a spectrum analyser, set-up for spectral measurements in the bandwidth of 0Hz-200 Hz, kept the same throughout these studies. Each spectrum was obtained with an r.m.s. (root mean square) of 25 averages for each spectrum, a Flat top or Hanning window was employed, which gave noise spectral resolutions of 1.9 Hz and 0.75 Hz respectively. The spectra ordinate axes were measured on the dB scale,

where $1\text{dB} = -20 \log V$ (where V is the signal amplitude).

The analytes studied were copper and magnesium as they are examples of anomalous and normal Zeeman splitting, respectively. These analytes were found to give the strongest signals for their type of Zeeman splitting.

Sample preparation

Diluted standard solutions were prepared from their respective 1000 ppm stock solutions, nebulised under optimised conditions and their analytical noise spectra were recorded. Blank measurements were performed with doubly distilled water, under the same conditions.

Results and Discussion

General features of the noise spectra

No sample present, Flame off:

Average white noise level (W_{av}) of the NPS consists of photon noise from the hollow cathode lamp (HCL) source in a given bandwidth. When the flame is turned on W_{av} is constant.

Analyte sample aspirated, Flame on:

Fluctuation noise begins to appear, dominating at frequencies below 300 Hz. Photon noise is also present. At concentrations near the detection limits background noise is mainly due to photon noise², above the detection limit background noise is mainly attributed to fluctuation noise. Interference peak frequencies also occur in the spectral range 0 Hz-200 Hz. These are the consequence of the spectrometer instrumentation and their origins are discussed below.

Fluctuation noise

In the measurement of analyte concentrations in a general spectrometric system, fluctuation noise originates from three sources:

(i) variation of the sample concentration aspirated into the flame system; this can be observed with concentration increase

(ii) fluctuation noise due to the change in refractive index in a hot flame¹²; this should be observable in the spectra of the blank solution

(iii) fluctuations in the transmission of light through the flame due to density variations of the vaporised sample; this should also give rise to fluctuation noise in the blank sample, and is more likely to affect absorption measurements^{1,13-16}.

Fluctuation noise may also arise from radiation sources (e.g., Xe arc lamps and laser sources). In this paper HCL sources were used which have negligible fluctuation noise contribution. Fluctuation noise occurs in the spectral range 0 Hz-300 Hz, and is recognised as a distinctive curve (called the $1/f$ curve) at low frequencies. As fluctuation noise increases the curve decays more slowly from 0 Hz and an increase in white noise level occurs per given bandwidth. With low fluctuation noise the spectra show no apparent $1/f$ curve only an increased average white noise level per given bandwidth. Fluctuation noise can, thus, be measured in two ways:

- a) The appearance and progression of the $1/f$ curve
- b) A proportional increase in average white noise level with concentration increase.

Interference Feature Frequencies

Two interference frequencies appeared with increase in analyte concentration. One of these was called a ‘flame’ interference frequency⁶, as it originated from parameters affecting the flame. It occurred within the range 15.5 Hz-39.0 Hz, its precise frequency depending on two parameters:

- (i) distance between the flame burner head and the optical path
- (ii) gas flow rate of air and acetylene.

Figures 2 and 3 show how these parameters affect the flame interference frequency. The figures suggest that this interference peak may be attributed to an “organ pipe” effect. As the flame gases move rapidly through the cooling sheets, it has a similar effect to a breeze and creates a very low frequency audio sound. Figure 3 also shows an interference frequency, which occurs at 100 Hz. This was called a ‘modulation’ interference frequency as it is thought to be generated by modulation of the atomic vapours magneto-optic properties. The source of this peak is ripple of about 10% fortuitously present on the electromagnet d.c. 50 Hz power supply⁶. This interference frequency was also observed by Bedenbender¹², but was attributed to ripple on the source power supply.

In Figure 2 a 50 Hz interference frequency is observable, which originates from the mains power supply of the hollow cathode lamp source, this frequency may be eliminated from subsequent spectra by the use of a battery power supply⁶ for the HCL source.

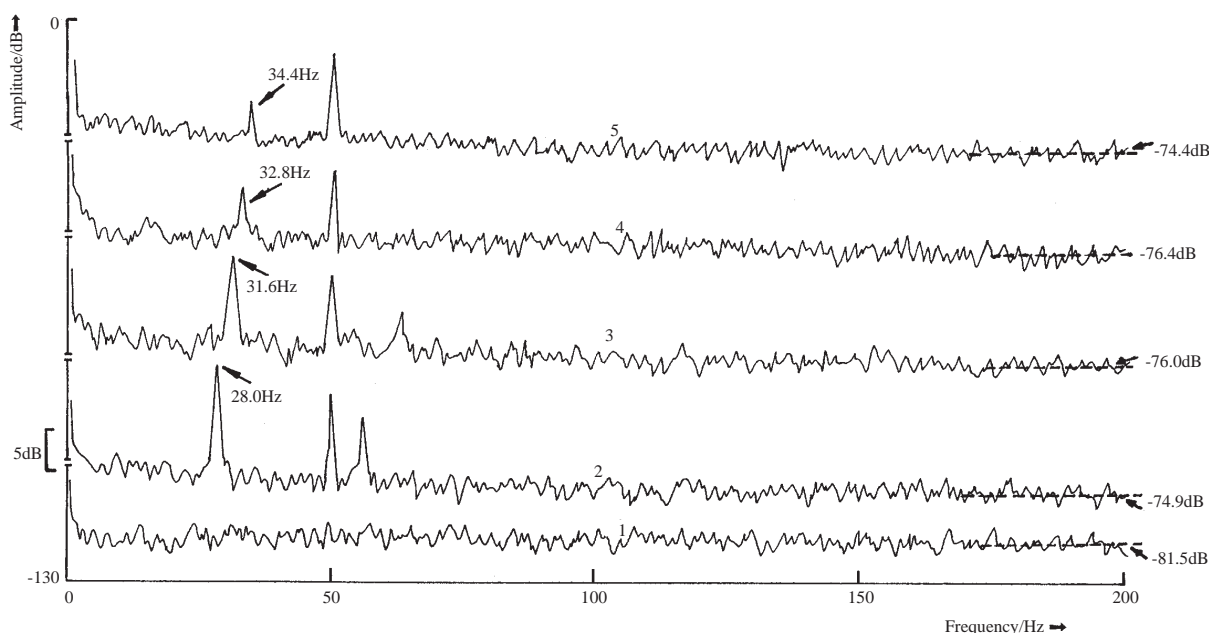


Figure 2. Variation of the flame frequency with flame burner distance (d_b) from the optical path, for the spectra of Ag in the crossed polariser configuration. Field strength; 0.27 T, concentration; 50 ppm, 1. Photomultiplier tube dark current, 2. $d_b=6.0$ cm, 3. $d_b=5.0$ cm 4. $d_b=4.0$ cm, 5. $d_b=2.0$ cm.

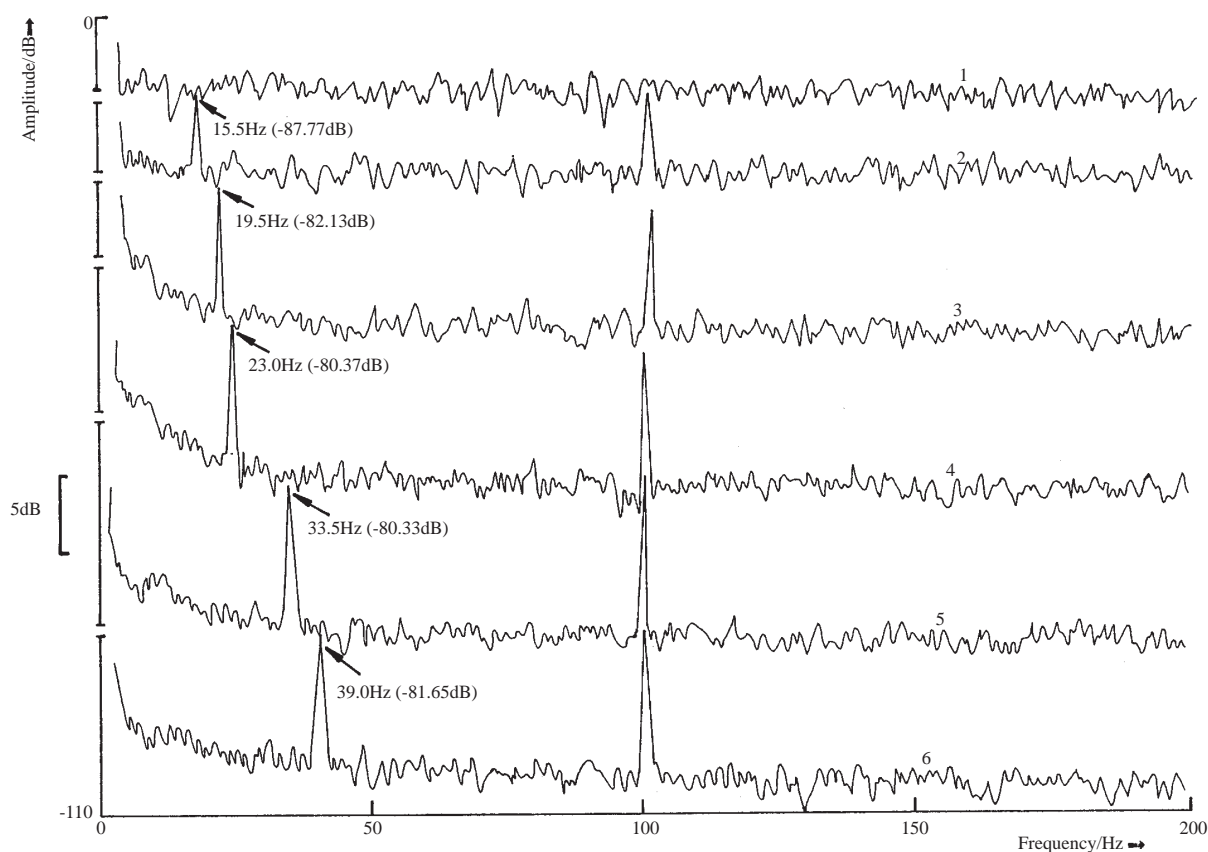


Figure 3. Variation of the flame frequency with ratio of air to acetylene (R) for the spectra of Mg using 45° offset polariser configuration, 0.55 T field strength, 30 ppm sample concentration and battery power supply for HCL. 1. Blank sample, 2-R=2.25, 3-R=2.6, 4-R=2.94 5-R=3.35, 6-R=3.53

Crossed polariser configuration $\Phi = 0^\circ$

Figures 4 (a) and 4 (b) show spectra of Mg and Cu. The lower spectrum of the blank with doubly distilled water aspirated indicates only photon noise. As concentration increases W_{av} increases, and at higher concentrations the $1/f$ curve is evident at the lower frequency end of the spectra. The $1/f$ curve is evident at 20 ppm in the Mg spectra, but only becomes evident at 150 ppm in the spectra of Cu. Thus, Cu spectra exhibit lower fluctuation noise compared with Mg spectra at a given concentration. Bedenbender¹² has attributed this to the fact that Cu releases fewer ionised particles in the air-acetylene flame than Mg (typical flame temperature ~ 2500 K). Thus, fluctuation noise must differ from element to element. The increase in fluctuation noise may be measured by the increase in the W_{av} as concentration increases and hence signal amplitude increases.

Figure 5 shows a plot of AMOR signal amplitude against W_{av} in the bandwidth of 0 Hz-200Hz. Both Cu and Mg graphs show a proportional increase of signal amplitude with W_{av} . However, for a given signal amplitude/concentration the Mg graph exhibits a higher amplitude of fluctuation noise than that of Cu.

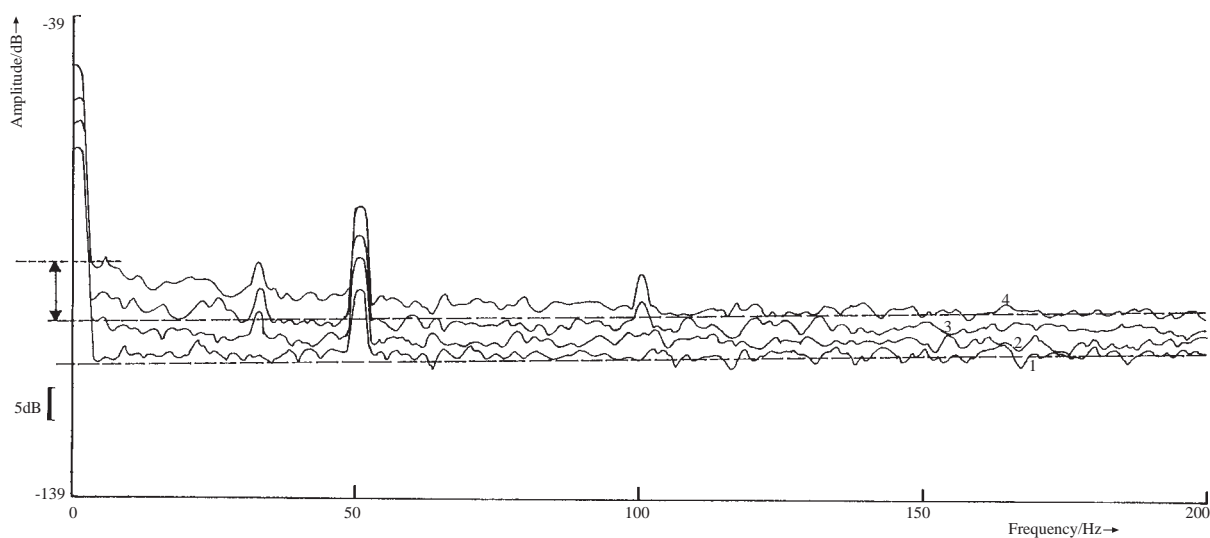
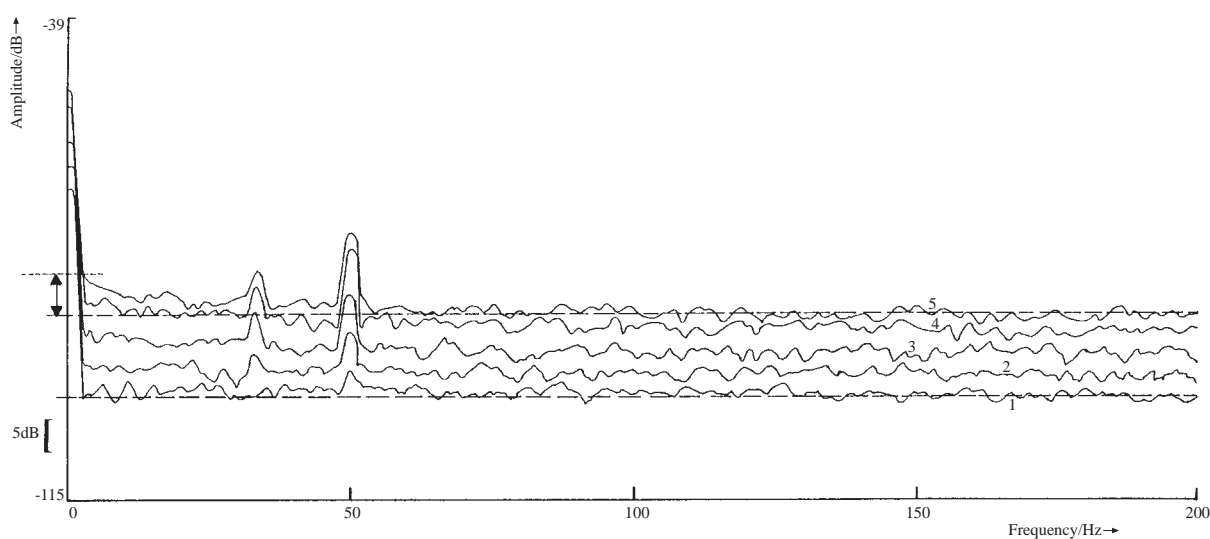


Figure 4. (a) Variation of fluctuation noise with concentration for the spectra of Mg using the crossed polariser configuration and 0.55 T field strength. 1. Leakage light through the crossed polariser, 2. 10 ppm, 3. 20 ppm, 4. 40 ppm, 5. 50 ppm.

(b) Variation of fluctuation noise with concentration for the spectra of Cu using the crossed polariser configuration and 0.22 T field strength. 1. Leakage light through the polariser, 2. 80 ppm, 3. 150 ppm, 4. 250 ppm.

Fluctuation noise is multiplicative. This can be observed by optimising the magnetic field in the AMORS measurements, and thereby higher output signal amplitudes. This result is observed in Figures 6 (a) and (b) for both Mg and Cu spectra at constant concentration, the fluctuation noise increases. Obtaining maximum signal-to-noise in the AMOR measurements thus requires optimisation of both magnetic field strength and source intensity.

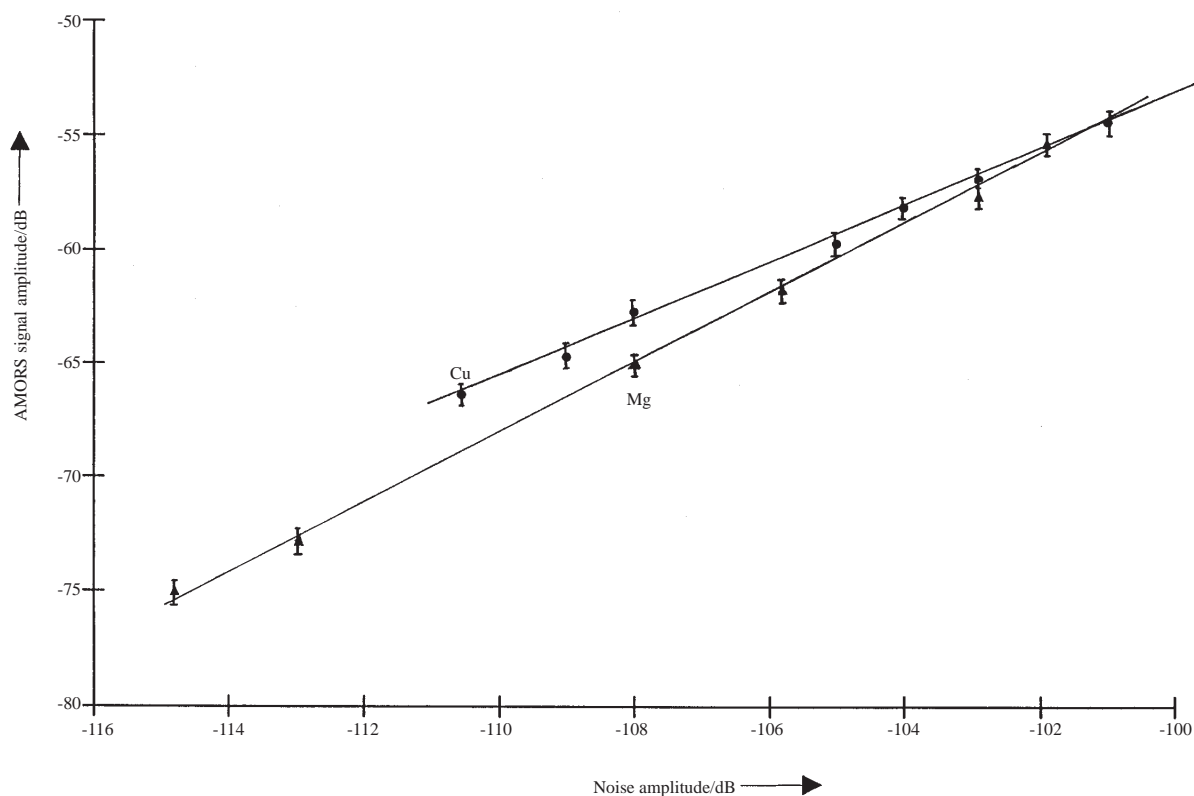


Figure 5. Fluctuation noise for Cu and Mg using the crossed polariser configuration in the bandwidth of 0 Hz-200 Hz.

Atomic Absorption (AA) Configuration

Figure 9 shows absorption spectra on channel A and B with no applied magnetic field. Fluctuation noise is slightly evident here at low concentrations, due to the initial large signal amplitude. As analyte concentration increases fluctuation noise decays.

Offset polariser configuration, $\Phi=45^\circ$

Offsetting the polariser by 45° allows all of the incident plane polarised light to be transmitted through the optical system and resolved by the analyser into two equal intensity orthogonally polarised beams^{5,6}, which carry both rotation and absorption information after interacting with the atomic vapour. These beams are focused above each other on the entrance slit of the monochromator and measured separately by two separate photomultipliers as shown in Figure 7. Figures 8 (a) and (b) show signal amplitude in channels A and B. Absorption of the incident light causes equal decreases in the signal amplitudes of channels A and B. However, rotation of the incident beam results in a signal of higher amplitude on channel A and a lower amplitude signal on channel B. Studies of the fluctuation noise were carried out over a range of concentrations on channel A and B output signals in the 45° offset polariser configuration using Mg as the analyte element. Both atomic absorption and AMOR configurations were studied, and the results are described below.

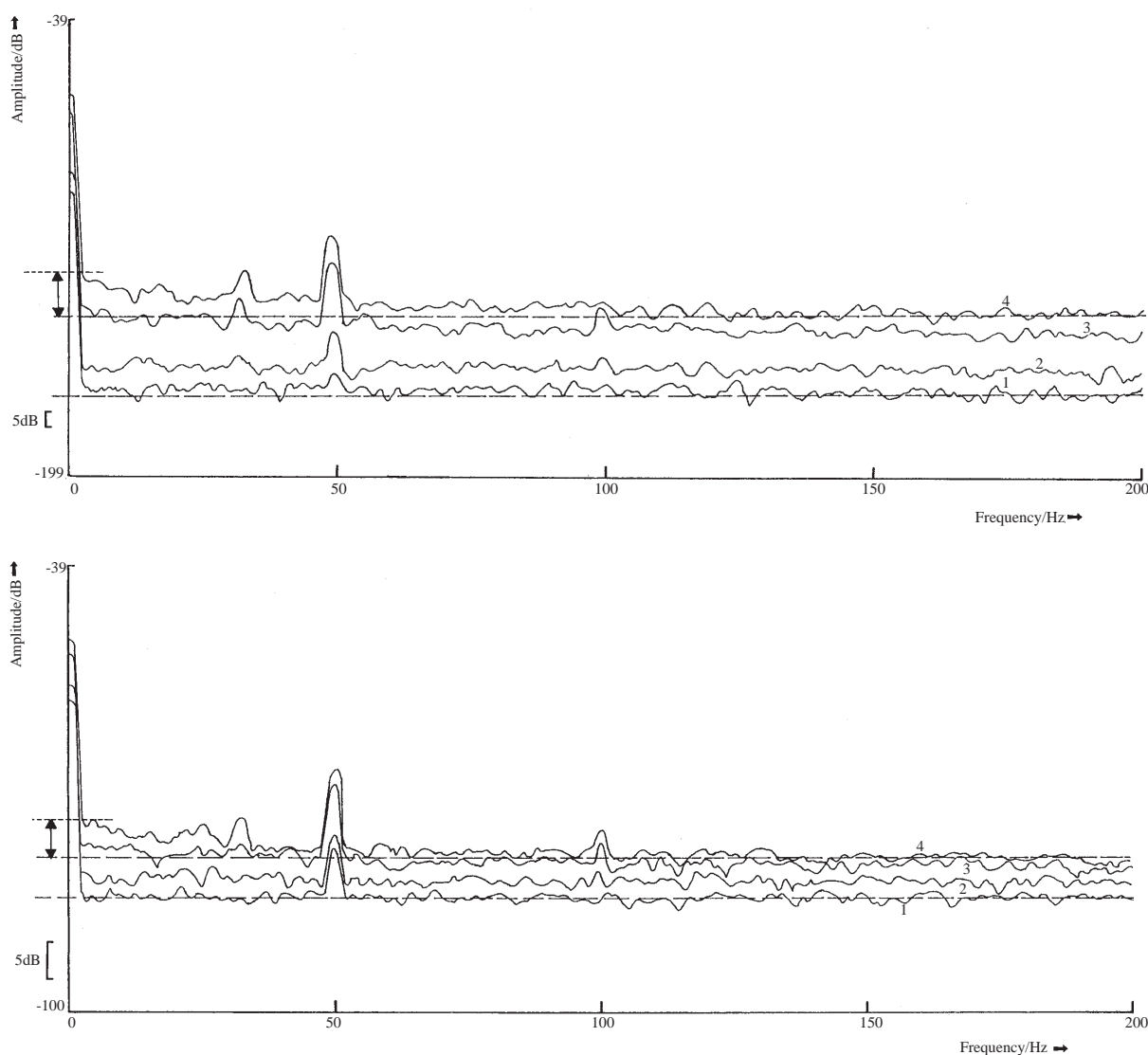


Figure 6. Variation of fluctuation noise with increased field strength in the crossed polariser configuration
 (a) for 50 ppm of Mg, 1. Leakage light (from the crossed polariser configuration), 2. 0.065 T, 3. 0.27 T, 4. 0.52 T.
 (b) for 150 ppm Cu, 1. Leakage light (from the crossed polariser configuration), 2. 0.01 T, 3. 0.06 T, 4. 0.22 T

AMORS Configuration

The spectra of Figures 10 (a) and (b) were obtained at an optimised magnetic field. No fluctuation noise was observed on the blank spectra. Fluctuation noise showed two different trends (especially below 20 Hz) as analyte concentrations increased. A chart-recorder (Kompensograph X-Y, 2 Hz bandwidth at the 3 dB point) was used to investigate this. The peak-to-peak amplitude of the fluctuation noise is plotted in figure 11 (a)-(c) for channel A and channel B. The fluctuation noise amplitude variations for channels A and B can be explained by considering Figure 8. At a given concentration, light is rotated towards channel A, so the latter always has a larger signal to noise ratio under a given set of conditions than channel B. In channel B the signal to noise ratio increases with concentration until 30 ppm and then decreases reaching a minimum at 80 ppm. Dichroic absorption occurred and virtually no signal reached the detector; as predicted by equation 1 the flicker noise amplitude decreased as a result.

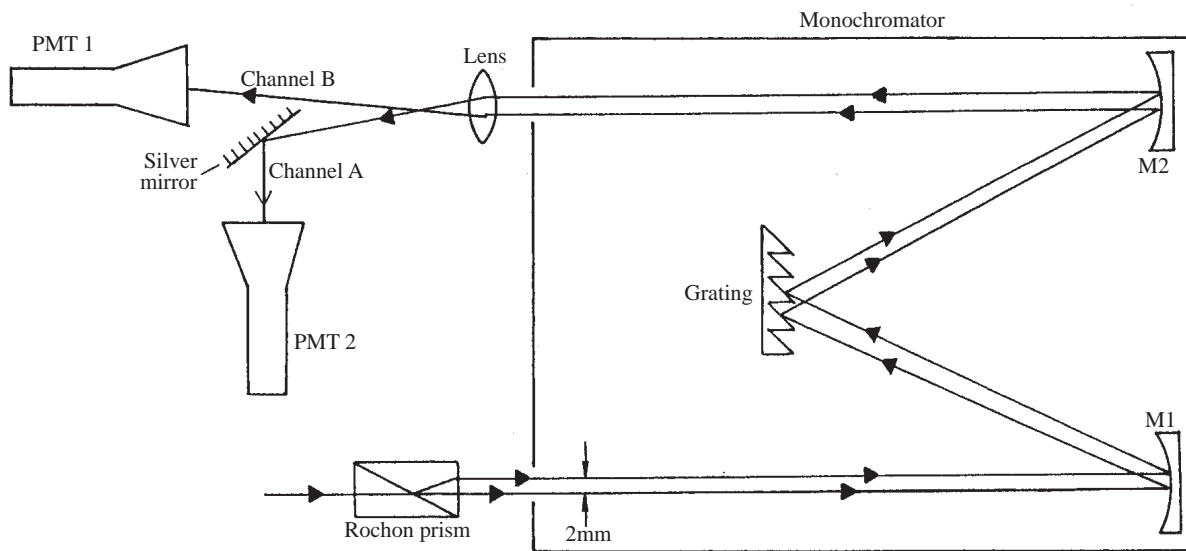


Figure 7. Measurement apparatus of AMORS using two photomultiplier tubes.

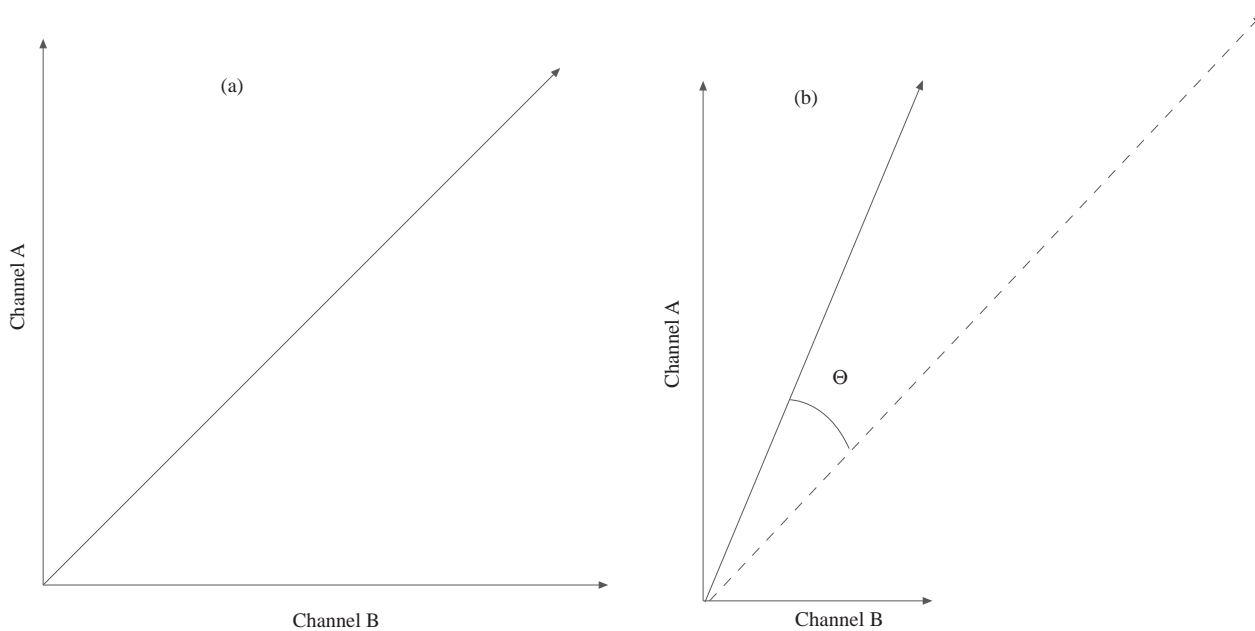


Figure 8. The result of absorption and rotation by the atomic vapour.

(a) Equal signal amplitude on channel A and B without analyte sample

(b) Signal amplitude on channel A and B, as result of absorption and optical rotation by atomic vapour.

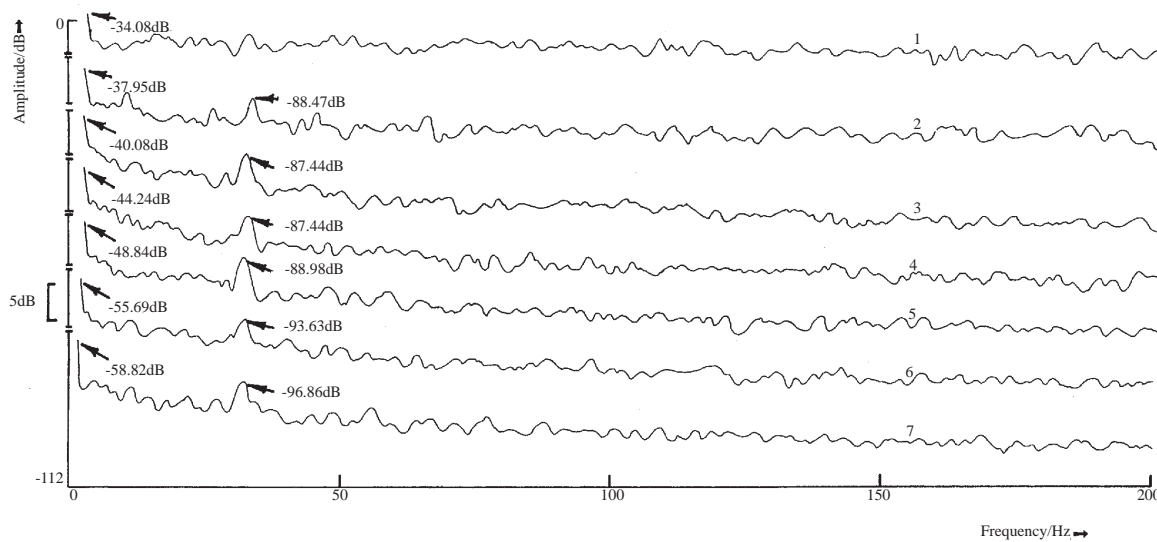
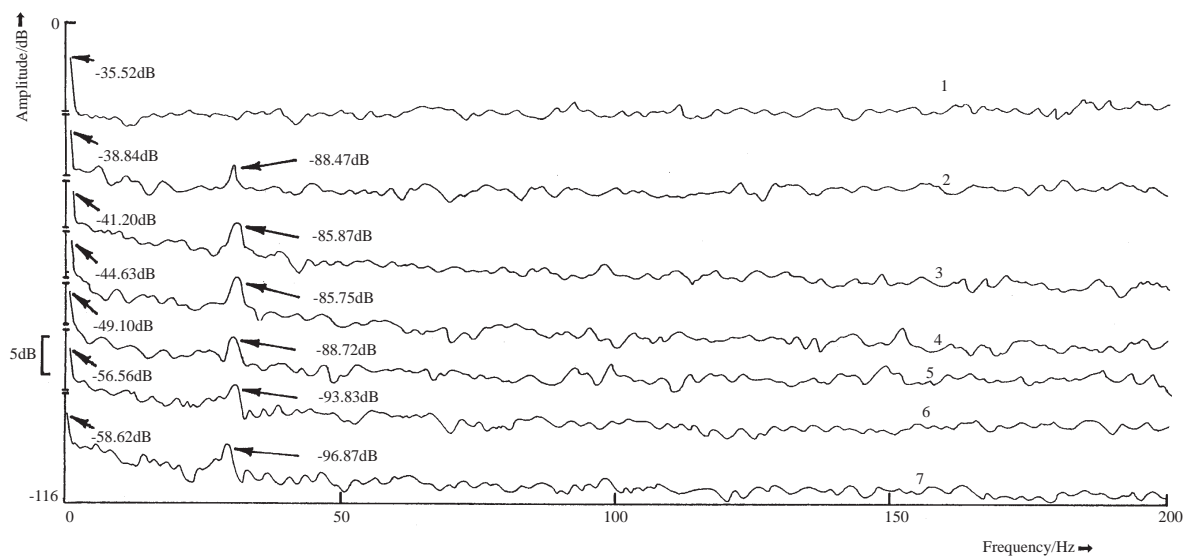


Figure 9. Atomic absorption mode in 45° offset polariser configuration (battery power supply used for HCL).

(a) Variation of d.c. signal amplitude with increased concentration of Mg on channel A. 1. Blank sample, 2. 10 ppm, 3. 20 ppm, 4. 30 ppm, 5. 50 ppm, 6. 80 ppm 7.100 ppm.

(b) Variation of d.c. signal amplitude with increased concentration of Mg on channel B. 1. Blank sample, 2. 10 ppm, 3. 20 ppm, 4. 30 ppm, 5. 50 ppm, 6. 80 ppm 7. 100 ppm.

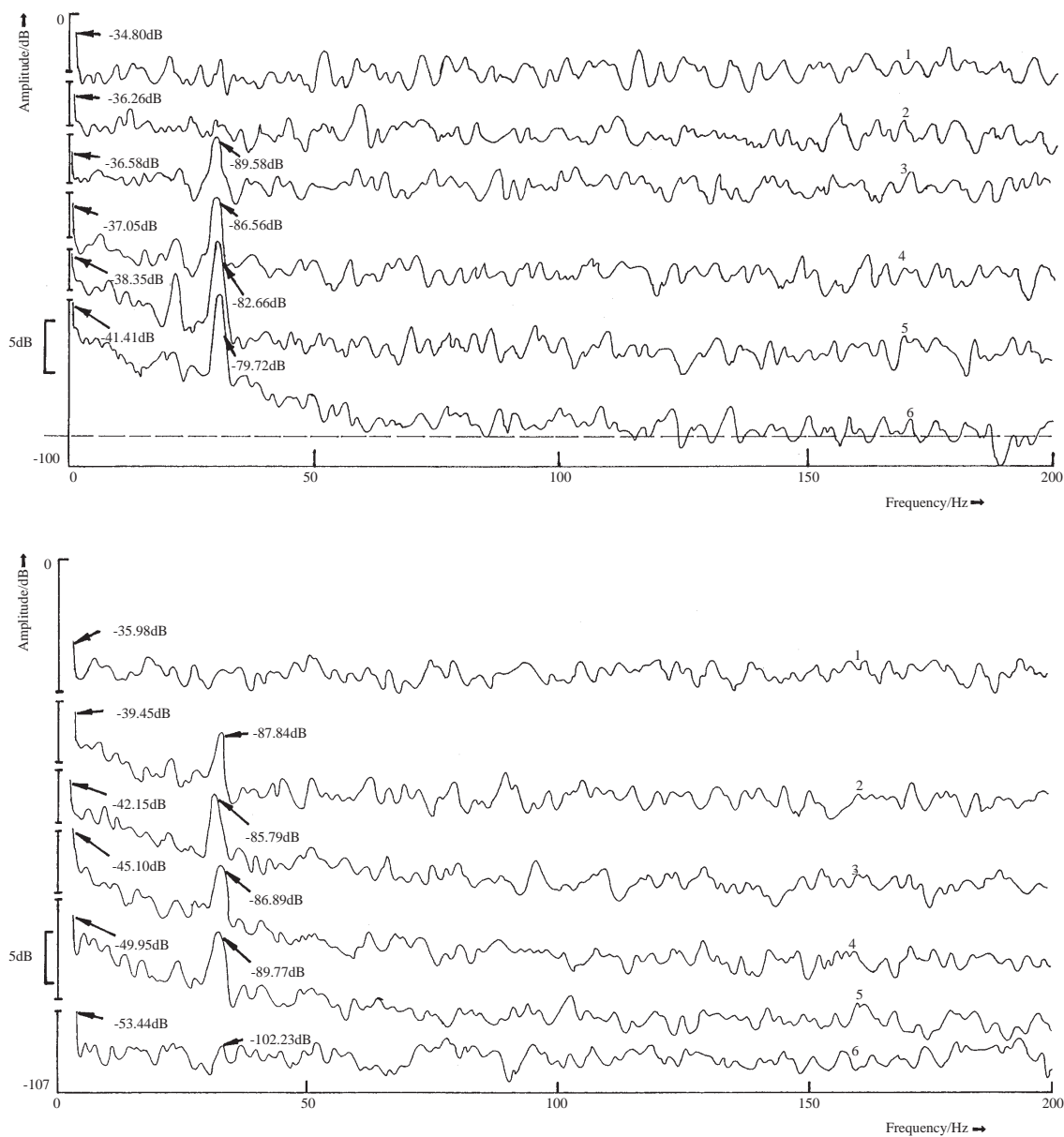
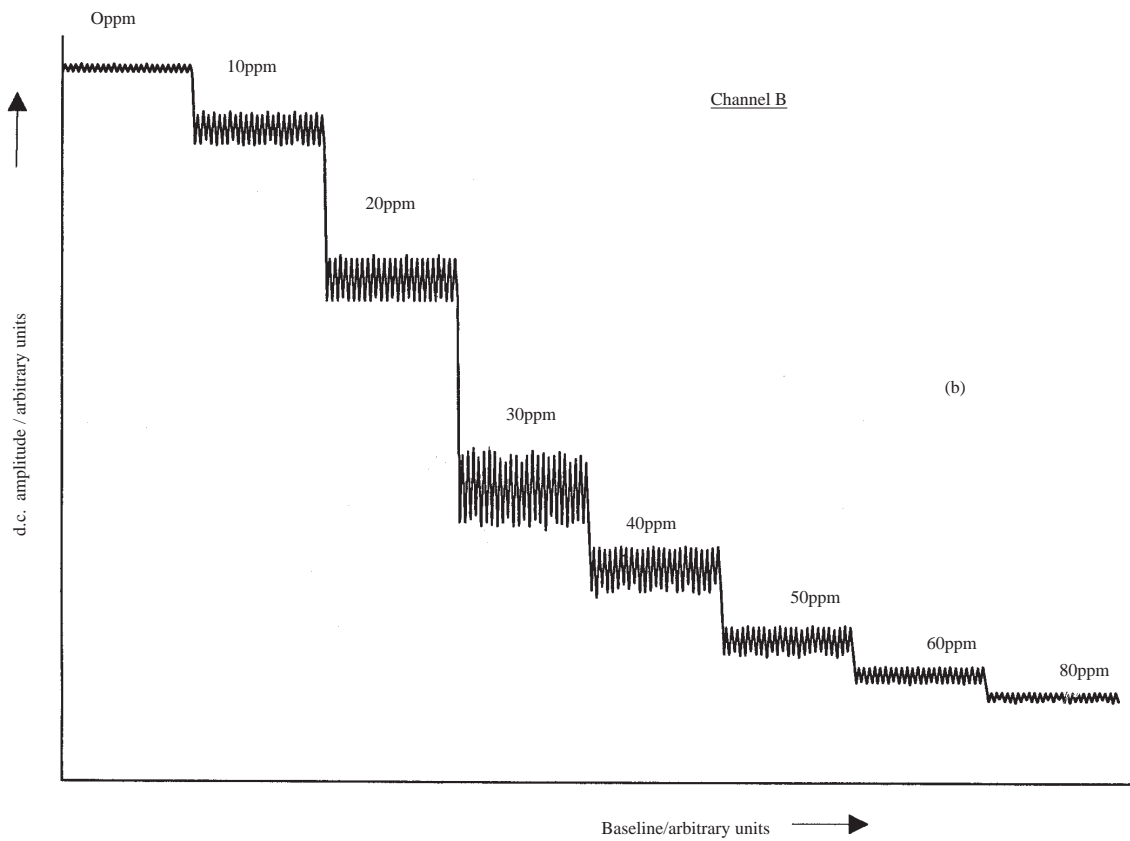
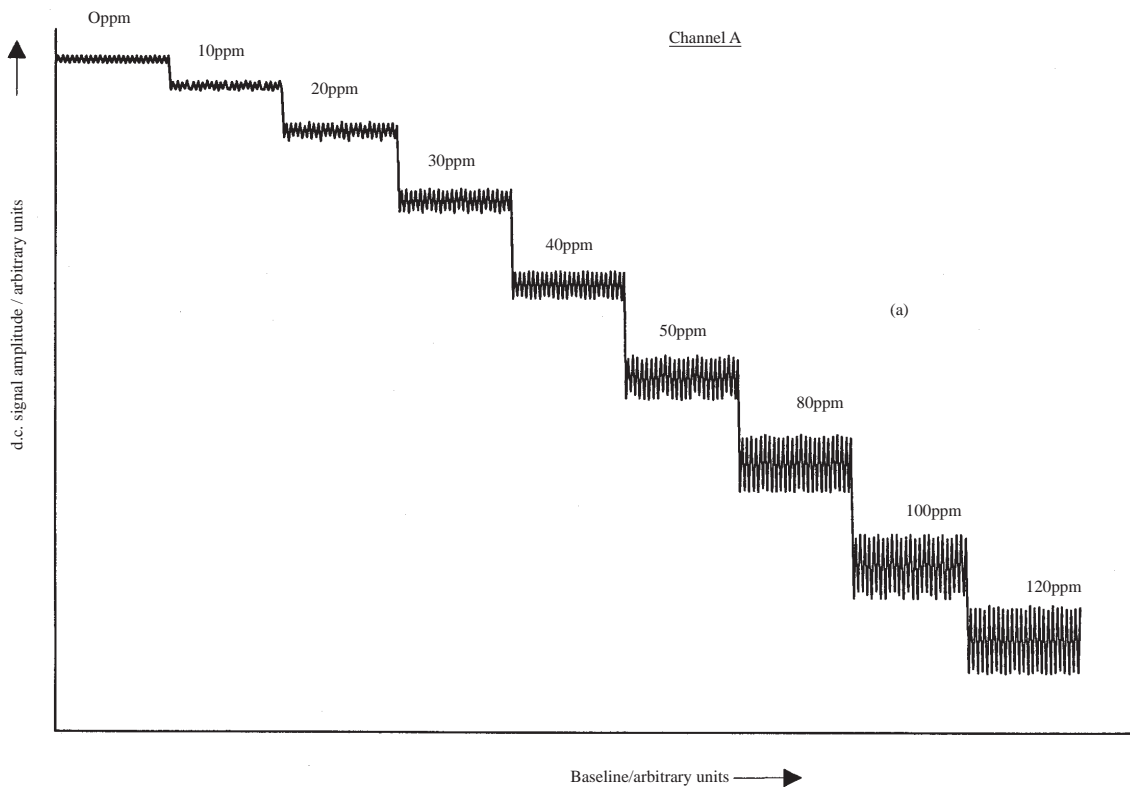


Figure 10. AMOR mode in 45° offset polariser configuration (battery power supply used for HCL).

(a) Variation of d.c. signal amplitude with increased concentration of Mg on channel A. 1. Blank sample, 2. 10 ppm, 3. 20 ppm, 4. 30 ppm, 5. 50 ppm, 6. 60 ppm.

(b) Variation of d.c. signal amplitude with increased concentration of Mg on channel B. 1. Blank sample, 2. 10 ppm, 3. 20 ppm, 4. 30 ppm, 5. 50 ppm, 6. 60 ppm.



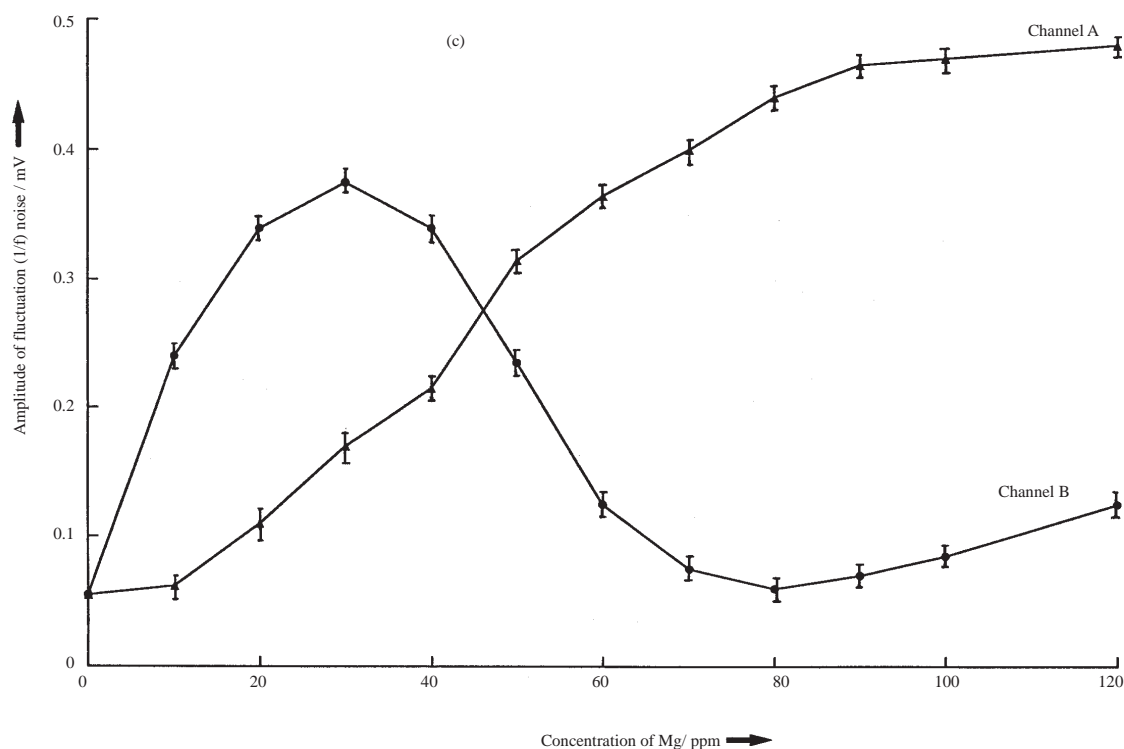


Figure 11. 1/f noise on the AMOR signal recorded by chart recorder in which the bandwidth of 0 Hz-2 Hz using 45° offset polariser configuration.

(a) Chart-recorder traces of 1/f noise in channel A.

(b) Chart-recorder traces of 1/f noise in channel B.

(c) Amplitude of fluctuation noise carried by the AMOR signal in the bandwidth of 0 Hz-2 Hz in channel A.

Conclusion

In AA and AMOR mode noise power spectra gave detailed information about noise sources in the instrumental measurement system. Fluctuation noise was found to vary from element to element, as was shown by comparing the spectra of Cu and Mg for given concentrations. It was proportional to the concentration of analyte in the AMORS crossed polariser configuration. In the 45° mode operated under two separate channels this was also the case for the absorption measurements, although in contrast to AMORS spectra fluctuation noise is present at low concentration here. In the AMORS 45° mode fluctuation noise showed a different trend. In this configuration the compensation effect of birefringent rotation was found to increase the signal-to-noise ratio in one channel, whilst reducing it in the other. This means that the channel having the highest signal to noise ratio may be chosen for analytical measurements.

The sources of two interference frequencies were identified. One was a flame interference frequency in the range 15.5Hz-39Hz which was attributed to an “organ-pipe” effect, arising from variation in the gas flow rates through the flame cooling sheets.

It is possible to vary the flame conditions to reduce this interference from the measurements. The second interference frequency is thought to arise from modulation of the AMORS signal.

References

1. P.R. Liddell, *Anal. Chem.*, **48**, No.13, p.1931, (1976).
2. A.T. Ince, R. D.Snook, and J. B. Dawson, *Anal. Proc.* **29**, p.59, (1992).
3. Hermann, G., Jung, G.M., Lasnitschka, G., Moder, R., Scharman, A., and Zhou, X., *Spectrochim. Acta, Part B*, **45**, p.763, (1990).
4. J. B. Dawson, P. R. King, R. J. Duffield and D. J. Ellis, *J.Anal. At. Spectrom.*, **4**, p.245, (1989).
5. J. B. Dawson, R. J. Duffield, A. D. Kersey, M. S. Hajizadeh and G. W. Fisher, *J.Anal. At. Spectrom.*, **2**, p.233, (1987).
6. A. T. Ince, Ph.D. Thesis, University of Manchester (UMIST), (1992).
7. A. D. Kersey, J. B. Dawson and J. D. Ellis, *Spectrochim. Acta, Part B*, **35**, p.865, (1980).
8. J. Kankare, R. Stephens, *Spectrochim. Acta, Part B*, **35**, p.849 (1980).
9. K. Kitagawa, W. Kuwayama, and Y. Ito, *Spectrochim. Acta. Part B*, **43**, p.481, (1988).
10. R. Stephens, *J.Anal. At. Spectrom.* **3**, p.227 (1988).
11. A. T. Ince, J. B. Dawson and R. D. Snook, *J.Anal. At. Spectrom.*, **11**, p.967, (1996).
12. H. Bedenbender, G. Hermann and A. Scharmann, *Spectrochim. Acta, Part B*, **45**, p.1225, (1990).
13. J. D. Jr. Ingle, *Anal. Chem.*, **46**, p.2161, (1974).
14. J. D. Winefordner, V. J. Vickers, *Anal. Chem.*, **37**, p.416 (1965).
15. M. L. Parsons, W. J. McCarthy and J. D. Winefordner, *J. Chem. Ed.* **44**, p.214 , (1967).
16. J. D. Winefordner, V. Svoboda and L. H. Chiue, *CRC Crit. Rev. Anal. Chem.*, (1970).